Characterization of the Redox and Metal Binding Activity of BsSco, a Protein Implicated in the Assembly of Cytochrome *c* Oxidase†

Iveta Imriskova-Sosova,‡ Diann Andrews, Katherine Yam, David Davidson, Brahm Yachnin, and Bruce C. Hill*

Department of Biochemistry, Queen's University, Kingston, Ontario, K7L 3N6 Canada

Received July 12, 2005; Revised Manuscript Received October 21, 2005

ABSTRACT: Members of the Sco protein family are implicated in the assembly of the respiratory complex cytochrome *c* oxidase. Several possible roles have been proposed for Sco: a copper delivery agent, a site-specific thiol reductase, and an indicator of cellular redox status. Two cysteine residues (C45 and C49) in the sequence CXXXCP and a histidine (H135) ~90 residues toward the C-terminus are conserved in Sco from bacteria, yeast, and humans. The soluble domain of Sco has a thioredoxin fold that is suggestive of redox activity for this protein. We have characterized the soluble domain of the Sco protein from *Bacillus subtilis* (i.e., sBsSco) for its redox reactivity and metal binding capacity. In oxidized sBsSco, the cysteines are present as an intramolecular disulfide. Oxidized sBsSco does not bind metal, but can be reduced in vitro to a metal-binding form. Reduction of the disulfide in sBsSco is accompanied by increased intrinsic fluorescence. The reducibility of the cystine is unchanged when the conserved histidine is mutated to alanine. Tight binding by reduced sBsSco is observed for Cu(II) by electronic absorption, intrinsic fluorescence, and EPR spectroscopies, and isothermal titration calorimetry with an observed stoichiometry of one Cu(II) ion per sBsSco and a K_D of ~50 nM. Tight binding of Cu(I) and Ag(I) is observed by quenching of intrinsic tryptophan fluorescence. Cobalt(II) exhibits weak binding, whereas Ni(II) and Zn-(II) do not appear to bind. The high-affinity binding of metals by BsSco is triggered by its redox state, and this property could be important for its function in vivo.

The heme−copper oxidases are a family of oligomeric, integral membrane enzymes that include mitochondrial cytochrome *c* oxidase, as well as cytochrome *c* and quinol oxidases from aerobic bacteria and aerobic archaea (*1*). Heme−copper oxidases catalyze the reduction of oxygen to water using electrons derived from reduced cytochrome *c* or quinol. Some of the free energy of the redox process is used to move protons across the membrane bilayer in a coupled proton transfer reaction. The most highly conserved features of members of the heme−copper oxidase family are found within the subunit I protein. Subunit I houses a binuclear heme−copper center that acts as the site of oxygen binding and reduction. The binuclear, oxygen reaction site is composed of a heme A moiety, known as cytochrome a_3, which is located ~5 Å from a copper center, known as Cu_B. The copper ion in the Cu_B center is ligated by three histidines, one of which is subjected to post-translational modification. Oxygen is proposed to interact with each of the metals of the cytochrome a_3−Cu_B center during the multistep process of O_2 binding and reduction (*2*).

In the cytochrome *c* oxidases, there are two other redox active centers that are involved in delivering electrons to the O_2-binding site defined by the cytochrome a_3−Cu_B center. One of the two is a second heme A moiety, known as cytochrome *a*, that is low-spin with both axial ligand positions occupied by histidine residues within subunit I. A second copper center, known as Cu_A, is found in the solvent-exposed domain of subunit II. This site has been shown to receive electrons from cytochrome *c* directly and is proposed to be the electron entry site for mitochondrial cytochrome *c* oxidase (*3*, *4*). The Cu_A site has two copper ions that are separated by bonding distance and are bridged by the thiol side chains of two cysteine residues within subunit II, in the sequence -**C**AEL**C**-.[1] A major difference between the cytochrome *c* oxidases and the quinol oxidases (e.g., cytochrome bo_3 or ubiquinol oxidase from *Escherichia coli*, and cytochrome aa_3-600 or menaquinol oxidase from *Bacillus subtilis*) is that the quinol oxidases do not have the Cu_A center in their otherwise similar subunits II.

The assembly of heme−copper oxidases is an inherently complex process (*5*). Multiple subunits are assembled within the membrane, and this is coordinated with the delivery and insertion of the redox active heme and copper ions. There are additional redox inert metals such as zinc and calcium that are also incorporated in the final structure. Specific accessory proteins have been implicated in the assembly of each of the four redox active centers of cytochrome *c* oxidases. In the model proposed for delivery of copper to cytochrome *c* oxidase, largely developed from studies in yeast (*6*, *7*), it is envisioned that copper is delivered to the two copper centers via different routes involving distinct

† This work was supported by an operating grant from the Natural Sciences and Engineering Research Council (Canada) to B.C.H. and an infrastructure grant from the Canadian Foundation for Innovation to the Protein Function Discovery group at Queen's University.

* To whom correspondence should be addressed. Phone: (613) 533-6375. Fax: (613) 533-2497. E-mail: hillb@post.queensu.ca.

‡ Current address: Department of Medical Genetics, 833 Medical Sciences Building, University of Alberta, Edmonton, AB, T6G 2H7 Canada.

[1] The sequence is from *B. subtilis* cytochrome *c* oxidase subunit II.

10.1021/bi051343i CCC: $30.25
Published on Web 11/30/2005

proteins. In the case of the Cu_A center, the small, soluble protein Cox17 was originally proposed to pick up copper in the cytosol, perhaps directly from one of the plasma membrane-bound copper pumps, and then to shuttle copper from the cytosol to the intermembrane space of the mitochondrial organelle (*8*). However, recent studies in which Cox17 was tethered to the inner mitochondrial membrane without a loss of functionality have drawn into question the shuttle role of Cox17 (*9*). Cox17 is proposed to be involved along with Sco[2] in the late stages of Cu_A assembly within aposubunit II of the oxidase. Cox17 could pass copper to the inner mitochondrial membrane-bound Sco protein, or directly to subunit II with Sco serving the function of maintaining the two Cu_A site cysteine thiols in a reduced state.

Sco was first characterized in yeast as a protein required for cytochrome *c* oxidase expression (*10*) and later proposed to participate in the delivery of copper to the oxidase (*11*). Metal analysis of the purified soluble domain of the yeast Sco1 protein reveals a stoichiometry of ~0.8 mol of copper/mol of Sco, and EXAFS[3] studies show that in these samples Cu(I) is bound to Sco via two cysteines and one histidine in a trigonal complex (*12*). Purified native Sco1 from yeast mitochondria contains 0.7−1 mol of copper/mol of Sco (*13*). In contrast, the protein purified from *B. subtilis* plasma membrane is almost copper free (i.e., <0.1 copper/BsSco) (*14*). Moreover, structural studies of the recombinant soluble domain of BsSco in solution (*15*) or in crystals (*16*), and crystals of the human protein (*17*), have not produced a structure for a metal-bound form of Sco.

To further delineate the possible functions of the Sco family of proteins, we have characterized the redox and metal binding properties of the Sco protein from the aerobic bacterium *B. subtilis*. We have taken advantage of the Cu-free form produced by our preparation of sBsSco to measure the strength and capacity of metal complex formation, which to date have not been quantified. The conserved cysteine pair of BsSco is redox active, although the reduced protein is relatively stable to oxidation by O_2 in vitro. The reduced protein binds both Cu(I) and Cu(II) with high affinity with a 1:1 stoichiometry. Nickel and zinc do not appear to bind, whereas cobalt forms a low-affinity 1:1 complex. These properties of BsSco are consistent with possible roles for this protein in the delivery of copper, and in sensing the metal or redox level of the cellular environment.

EXPERIMENTAL PROCEDURES

sBsSco was purified from *E. coli* as described previously (*18*). The mutant of sBsSco with His135 changed to Ala was generated as described previously (*16*). The standard buffer used in all the experiments reported here was 50 mM sodium phosphate (pH 7.0) that had been passed over a Chelex (Sigma) column to remove any trace metal ion contamination. The metal ions were used as the following salts: $CuCl_2$, $AgNO_3$, $ZnCl_2$, $CoCl_2$, and $NiCl_2$. Stock solutions of Cu(I) were prepared fresh by stoichiometric addition of glutathione, DTT, or TCEP to a solution of $CuCl_2$ under an atmosphere of argon in a Thunberg cell (*19*). Reduction of sBsSco was achieved by incubation with 1−2 mM DTT for 1−2 h at 20 °C. Excess DTT was removed by gel filtration over G-25 Sephadex, or by ultrafiltration using a 5 kDa cutoff filter. All reagents were the purest grade commercially available.

Fluorescence spectroscopy was performed on a Fluorolog-3 spectrometer from Horiba Jobin-Yvon. Emission intensity data were collected with excitation at either 280 or 295 nm, with the excitation slit set at 1 nm and the emission slit set at 2 nm. Absorption spectra were obtained on either a Hewlett-Packard 8452A diode array or a Cary-50 spectrophotometer. For each reported fluorescence determination, the absorption spectrum was determined over the appropriate range so that inner filter effects (*20*) on the fluorescence emission could be corrected.

EPR spectra were collected on a Bruker EMX spectrometer fitted with an Oxford Instruments ESR9 flow cryostat. Power saturation experiments were conducted between 20 and 120 K to determine the relaxation properties of the Cu(II)−sBsSco complex. Spectra were recorded under nonsaturating conditions at 80 K with a power of 2 mW. Quantification of the spin system of the Cu(II)−sBsSco complex was done by double integration in comparison to a sample of the Cu−EDTA species run under the same conditions. This method shows that our reconstitution of copper with reduced apo-sBsSco yields, within experimental error, complete formation of a 1:1 Cu(II)−sBsSco complex. Spectral simulations were done using the SimFonia software from Bruker that is able to account for anisotropy of the *g* value as well as nuclear and ligand hyperfine splitting. The simulation parameters are given in Figure 5.

Isothermal titration calorimetry data were collected on a MicroCal VP-ITC instrument. The temperature for all titrations was 30 °C. The protein sample was in the reaction cell, and the ligand to be added was in the titration syringe. The protein and ligand sample solutions were degassed thoroughly prior to loading the calorimeter. ITC data were analyzed with the processing software supplied by MicroCal using the Origin package. The plot of heat change at each ligand concentration was fit to a model specifying a single type of binding site to obtain the equilibrium constant, enthalpy change (ΔH), and stoichiometry.

Sedimentation velocity data were collected on a Beckman Optima XL-I ultracentrifuge. The protein concentrations were close to 0.2 mg/mL in each case. The runs were conducted at a speed of 55 000 rpm, and at 20 °C. The concentration profiles across the cells were monitored over time by scanning in absorbance mode at 280 nm. Analysis was done using SEDFIT (*21*).

RESULTS

Redox Reactivity of the Cysteine Pair of BsSco. BsSco has two available cysteine residues in the mature, native protein, and in the soluble domain described here. We have employed the thiol reactive reagent 4,4-dipyridyl disulfide (*22*) to determine the content of reduced and reactive cysteine residues in sBsSco. Our preparation of purified sBsSco results in a nearly fully oxidized protein with 0−0.2 mol of

[2] Sco nomenclature: Sco, Sco family of proteins; BsSco, Sco protein from *B. subtilis*; sBsSco, soluble domain of BsSco; sBsScoHA, mutant of sBsSco in which His135 has been changed to alanine.

[3] Abbreviations: DTT, dithiothreitol; EDTA, ethylenediaminetetraacetic acid; EPR, electron paramagnetic resonance; EXAFS, extended X-ray absorption fine structure; ITC, isothermal titration calorimetry; TCEP, tris(2-carboxyethyl)phosphine; TRX, thioredoxin.

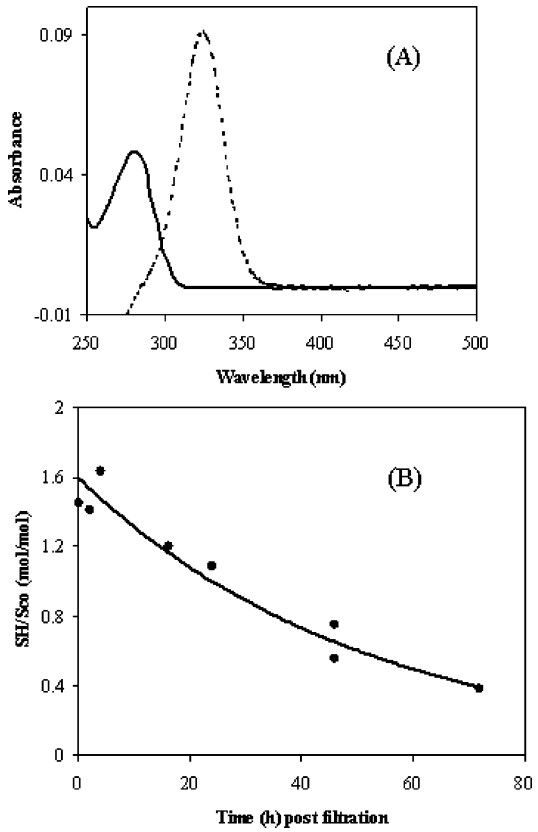

FIGURE 1: Detection of available thiol groups in sBsSco. A solution of 5.12 μM sBsSco was placed on one side of a split cuvette. A spectrum was recorded with buffer on the other side to determine the protein concentration. To the buffer side was added 1 μL of 50 mM 4,4′-dithiopyridine, and spectra were recorded over time (~10 min) to determine the background rate of hydrolysis. The contents of the two sides were mixed, and recording was continued to assess the extent and rate of thiol reactivity of sBsSco. (A) The solid line is the spectrum of sBsSco referenced to buffer. The dotted line is the spectrum obtained following mixing of the contents of the two compartments of the split cuvette with the spectrum before mixing taken as the reference. The extinction coefficient for sBsSco at 280 nm is 19.2 mM^{-1} cm^{-1} and for thiopyridone 18.8 mM^{-1} cm^{-1}. The ratio of thiol to sBsSco obtained from this sample is 1.90. (B) A sample of reduced sBsSco was left in air at room temperature, and at the indicated times, the thiol content was determined as described above.

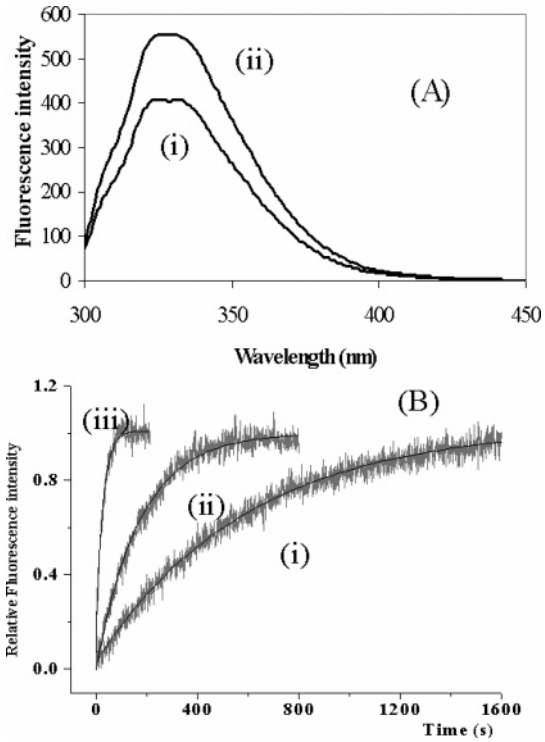

FIGURE 2: Intrinsic protein fluorescence and kinetics of reduction of sBsSco by dithiothreitol. (A) Emission spectra of oxidized (i) and DTT-reduced (ii) sBsSco. The concentration of sBsSco was 4.95 μM in each trace, and reduction was achieved by treatment with 1 mM DTT. The buffer was 50 mM sodium phosphate (pH 7.0), and the temperature was 20 °C. The excitation wavelength was 280 nm, the excitation band-pass 1 nm, and the emission band-pass 2 nm. (B) Time courses for the fluorescence change of sBsSco induced by the addition of excess DTT. The concentration of sBsSco was 2.5 μM, and the DTT concentrations were (i) 90 μM, (ii) 280 μM, and (iii) 2.80 mM. The line through the data is the single-exponential fit from which the observed rate of reduction was obtained. Other experimental conditions were the same as outlined above.

free cysteine/mol of protein, and this number is unchanged when sBsSco is denatured. Previous work has shown that in oxidized sBsSco the cysteine pair is in an intramolecular disulfide (*16*). When oxidized sBsSco is treated with either of the reducing agents, DTT or TCEP, and the excess reducing agent removed by gel filtration, up to 2 mol of thiol (1.85 ± 0.18, $n = 7$) is detected per mole of protein (Figure 1A). Once the protein is reduced, its return to the oxidized state under the conditions used here is slow. The half-life of reduced sBsSco at neutral pH and room temperature is 32 h (Figure 1B).

Intrinsic Fluorescence and Redox Kinetics of sBsSco. In many members of the thioredoxin family, intrinsic protein fluorescence has proven to be a sensitive and useful indicator of the status of the redox active cysteine pair (*23*, *24*). This is due to the highly efficient quenching of tryptophan fluorescence by the disulfide-bonded, cystine residue (*25*). BsSco has two conserved cysteine residues that are key to its function in vivo (*26*), and in our preparations of sBsSco are oxidized in an intramolecular disulfide. We sought, therefore, to characterize the intrinsic fluorescence of sBsSco to determine if its redox state could be monitored using the protein's fluorescence. sBsSco has two tryptophan and eight tyrosine residues, and when excited at either 280 or 295 nm, sBsSco has an emission maximum at 330 nm that is typical for protein fluorescence arising primarily from tryptophan (Figure 2A). There is also a shoulder centered at 310 nm, even after correcting for the contribution due to Raman scattering of the aqueous buffer, that is slightly more pronounced when excitation is at 280 nm compared to when excitation is at 295 nm. This is consistent with the 310 nm component of the spectrum arising from a contribution from tyrosine. It is often the case in proteins containing both tryptophan and tyrosine that a distinct contribution from tyrosine is difficult to detect due to the higher absorption and quantum yield of tryptophan, and/or due to efficient energy transfer from tyrosine to tryptophan. The 310 nm feature of the emission spectrum of sBsSco is a feature of the native protein as it disappears upon denaturation.

The intrinsic fluorescence of sBsSco increases upon addition of DTT (Figure 2A), and the rate of this increase is proportional to the reductant concentration as illustrated for a few DTT concentrations (Figure 2B). A plot of the observed reduction rate of sBsSco versus DTT concentration

Table 1: Second-Order Reduction Rates for BsSco and Thioredoxin[a]

protein	reduction rate (M^{-1} s^{-1}) DTT	TCEP	ref
SBsSco	20.1 ± 2.58	0.341 ± 0.093	this work
sBsScoHA	17.2 ± 1.68	0.443 ± 0.091	this work
E. coli TRX	1650	−	*23*

[a] Reactions were started by mixing a small aliquot of DTT with ~5 μM sBsSco.

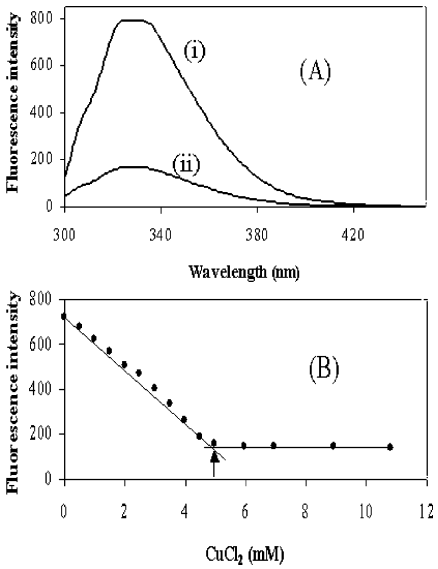

FIGURE 3: Measurement of the extent of binding of Cu(II) to reduced sBsSco by intrinsic fluorescence. (A) Intrinsic fluorescence of reduced sBsSco (i) and the level obtained after the addition of 20 μM $CuCl_2$ (ii). The concentration of reduced apo-sBsSco was 5.83 μM. The experimental and instrumental conditions were otherwise as outlined in the legend of Figure 2. (B) Titration of the copper-induced fluorescence change. The fluorescence intensity was measured at 330 nm following each addition of copper. The fluorescence level was followed vs time after each addition to ensure that equilibrium was established prior to the next addition. There is a sharp discontinuity in the fluorescence decline indicated by the arrow. Further addition of copper results in no further fluorescence change. The break point in this case occurs at a $CuCl_2$ concentration of 5.05 μM at a ratio of 0.92 Cu(II) to sBsSCO.

is linear with a slope, corresponding to the bimolecular rate constant, of 20.1 ± 2.58 M^{-1} s^{-1} (Table 1). The rate of bimolecular reduction of sBsSco by DTT is 80-fold slower than that reported for thioredoxin from *E. coli*. As expected, a similar emission increase is observed when the phosphine-based reducing agent, TCEP, is used. The reactivity of oxidized sBsSco, however, is slower with TCEP than with DTT, although TCEP is a thermodynamically stronger reducing agent. The slower reactivity of sBsSco with TCEP compared to DTT may reflect the steric hindrance of the disulfide site in sBsSco toward the bulkier TCEP molecule (*27*).

Spectroscopic Characterization of the Reaction of sBsSco with Copper. Addition of $CuCl_2$ to previously reduced apo-sBsSco results in quenching of the protein's intrinsic fluorescence by ~80% (Figure 3A), whereas addition of $CuCl_2$ to oxidized apo-sBsSco or to mutants of sBsSCO in which either Cys45 or Cys49 is changed to Ser or His135 is changed to Ala causes no change. The shape of the emission spectrum of sBsSco is unchanged upon copper binding, consistent with lack of a large-scale protein conformational change upon formation of the metal−protein complex. Although the putative copper ligands (Cys45, Cys49, and His135) are too far apart in the crystal structure of sBsSco (*16*) to bind a metal ion, only small structural changes are required to allow a binding site to form. When the Cu(II)-induced, fluorescence change is used to measure the affinity of copper binding, the magnitude of the fluorescence decrease is linear as the copper concentration increases until a sharp break point is reached, after which further copper addition causes no change (Figure 3B). The break point was determined to be at 0.94 ± 0.54 Cu(II) per sBsSco in three independent experiments. The addition of EDTA in excess does not reverse the fluorescence decline induced by copper on a time scale of minutes. This is probably a reflection of the slow rate of dissociation of Cu(II) from the Cu(II)−sBsSco complex rather than the fact that sBsSco has a higher binding constant for copper than EDTA. These data are consistent with formation of a high-affinity 1:1 complex between reduced apo-sBsSco and copper(II).

Equilibrium binding of Cu(II) to reduced apo-sBsSco was also monitored by absorption spectroscopy. Addition of Cu(II)Cl_2 to reduced sBsSco gives rise to an absorption spectrum with peaks at 354, 456, and 552 nm with the most intense absorption band at 354 nm having an extinction coefficient of 4.78 ± 0.45 mM^{-1} cm^{-1} (Figure 4A). When formation of the UV−vis absorption spectrum is used to follow the binding of copper to reduced sBsSco (Figure 4B), the form of the titration shows a linear increase in absorption with incremental additions of $CuCl_2$ until a maximum absorption is obtained, after which there is no further increase (Figure 4C). The break point occurs in this example at a $CuCl_2$ concentration of 9.5 μM and a Cu(II):sBsSco ratio of 0.90. This ratio was determined in three separate experiments to give an average value of 0.95 ± 0.05 and is consistent with formation of a 1:1 complex of sBsSco with Cu(II). The features of this absorbance-based titration mirror those obtained when using fluorescence change to monitor copper binding.

We have used EPR spectroscopy to confirm the redox state of the copper that is present in the complex formed with reduced sBsSco. Figure 5A shows EPR spectra for reduced apo-sBsSco and after addition of 1 equiv of $CuCl_2$. Addition of $CuCl_2$ to apo-sBsSco gives rise to an EPR spectrum with features of copper(II). When more than 1 equiv of $CuCl_2$ is added to apo-sBsSco, a second form of copper can be detected by EPR, and it is similar to the signal observed when $CuCl_2$ is added to buffer alone. Power saturation studies of the Cu(II)−sBsSco complex from 20 to 120 K show that the features of the spectrum arise from the same spin system. The EPR spectrum of the Cu(II)−sBsSco complex is shown in more detail and at higher concentrations in Figure 5B. The copper site exhibits a rhombic character, with a g_z of 2.170 and metal hyperfine splitting (A_z = 178 G), consistent with metal−thiolate ligation (*28*). The g_x and g_y terms do not differ by much, and metal hyperfine splitting is observed on both of these two higher-field transitions. In addition, broadening of the spectral lines indicates the presence of nonresolved ^{14}N−ligand hyperfine interactions from the histidine side chain. Further work is underway to understand the details of this spectrum, but it does illustrate that the addition of Cu(II) to reduced apo-sBsSco does not result in

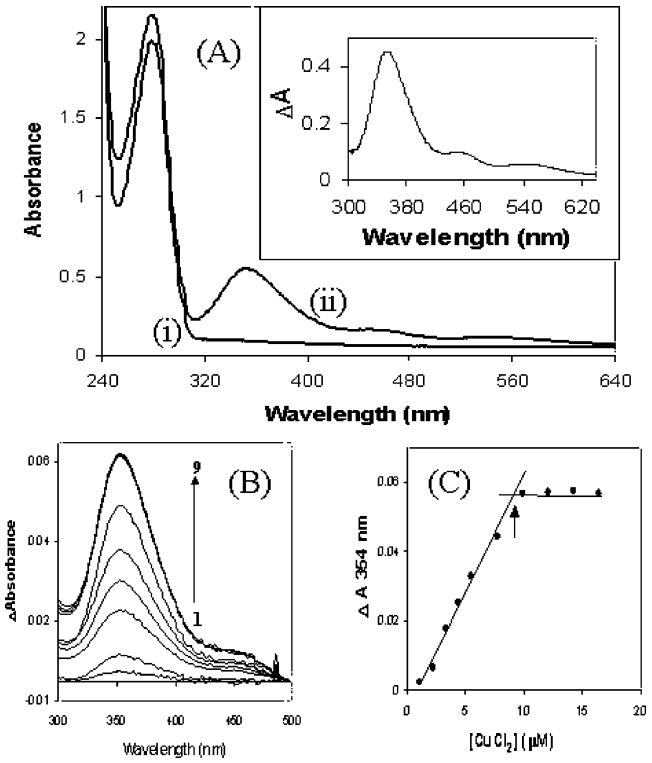

FIGURE 4: UV−visible absorption of sBsSco and its complex with Cu(II). (A) Absolute absorption spectra for apo-sBsSco and the Cu(II)−sBsSco complex. The concentration of sBsSco was 99.5 μM with $CuCl_2$ concentrations of 0 (i) and 100 μM (ii). The inset shows a blow-up of the difference spectrum of Cu(II)-bound sBsSCO with apo-sBsSCO as a reference from 300 to 640 nm. (B) Difference spectra generated by the addition of $CuCl_2$ to apo-sBsSco. The spectrum of the apoprotein was used as a reference and was subtracted from the spectrum at each copper concentration. The concentration of reduced sBSco was 11 μM, and spectra 1−9 correspond to increasing concentrations of $CuCl_2$. The final concentrations of $CuCl_2$ for each spectrum were (1) 1.11, (2) 2.21, (3) 3.32, (4) 4.42, (5) 5.52, (6) 7.71, (7) 9.92, (8) 12.2, and (9) 14.6 μM. (C) Plot of the change in absorbance at 354 nm vs copper concentration. The data are from panel B. The experiments were conducted at 20 °C, and the buffer was 50 mM sodium phosphate (pH 7.0).

copper reduction but instead leads to a protein complex with oxidized copper. The features of this spectrum disappear upon reduction by sodium dithionite, as the reduced (d_{10}) Cu(I) ion is EPR silent. Furthermore, when $CuCl_2$ is added to oxidized apo-sBsSco, a spectrum that is identical to that of $CuCl_2$ added to buffer alone is observed, consistent with the requirement that the disulfide site on BsSco be reduced for high-affinity metal binding.

ITC Characterization of Binding of Copper to sBsSco. Isothermal titration calorimetry has been used to quantify the energetics of sBsSco's interactions with metal ions. Figure 6 shows the results of titrations of reduced and oxidized apo-sBsSco with $Cu(II)Cl_2$. In panel A, the amount of power (microcalories per second) used at each injection is plotted versus time for the titration of reduced sBsSco with $Cu(II)Cl_2$, and for a titration of oxidized sBsSco with $Cu(II)Cl_2$. For the titration of reduced sBsSco with copper, the first injection gives a small response that is, presumably, a result of the loss of some titrant out of the tip of the syringe during the incubation period prior to the start of the titration. Following the first injection, there are a series of deflections that are similar for each injection. This corresponds to a

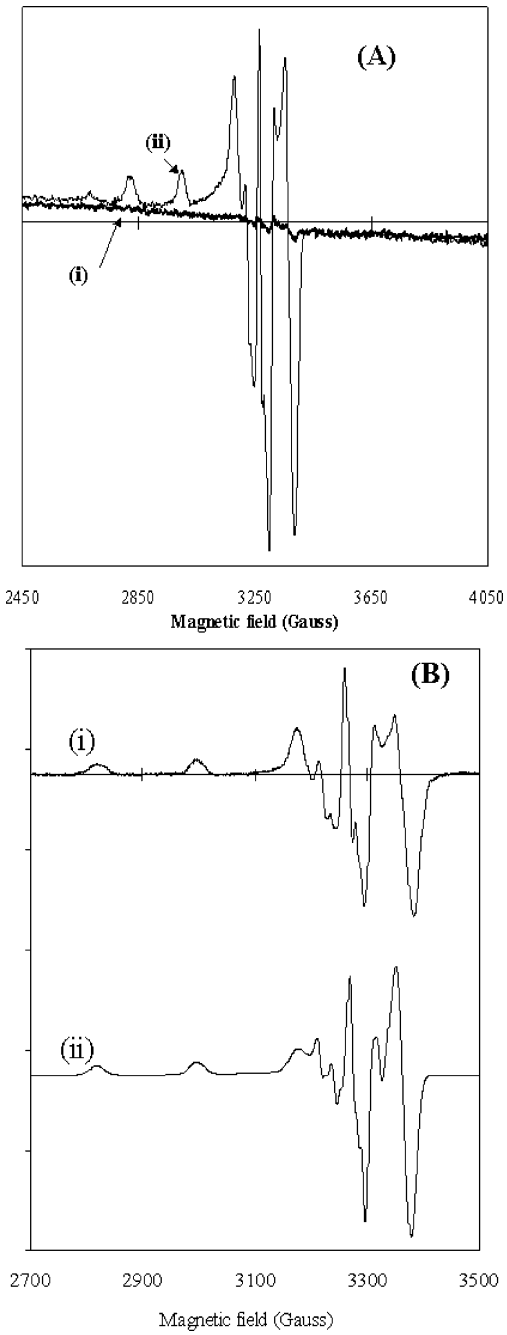

FIGURE 5: EPR spectroscopy of sBsSco bound with $Cu(II)Cl_2$. (A) EPR spectra for apo-sBsSco (i) and apo-sBsSco with 1 equiv of $CuCl_2$ (ii). The concentration of sBsSco was 35.0 μM, and the concentration of added copper was 33 μM. The EPR conditions were as follows: microwave frequency, 9.362 GHz; power, 2 mW; modulation amplitude, 4 G; and temperature, 80 K. (B) (i) EPR spectrum of the copper(II)−sBsSco complex. The protein concentration was 99.5 μM, and the concentration of added copper was 100 μM. EPR conditions were as follows: microwave frequency, 9.371 GHz; power, 2 mW; modulation amplitude, 4 G; and temperature, 80 K. The spin intensity of the Cu(II)−sBsSCO complex was quantified by reference to a Cu−EDTA standard. (ii) Simulation of the Cu(II)−sBsSco spectrum. The parameters for the simulation were as follows: $g_x = 2.048$, $g_y = 2.066$, and $g_z = 2.170$ with hyperfine splitting of $A_z = 25$ G, $A_y = 45$ G, and $A_z = 178$ G. The simulation was done using Simfonia (Bruker).

portion of the binding curve in which the concentration of added ligand is well below saturation so each addition of ligand produces a similar signal increment. Such a result is found in tight binding interactions even as saturation is

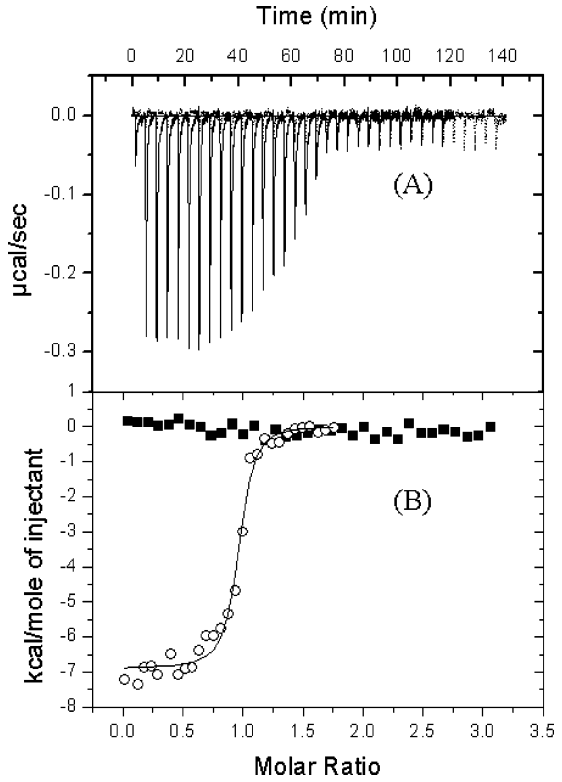

FIGURE 6: Isothermal titration calorimetry to assess the binding of Cu(II) to apo-sBsSco in the reduced and oxidized states. (A) The power (microcalories per second) is plotted vs time over the titration. Each downward deflection corresponds to the injection of an aliquot of Cu(II)Cl_2. The solid trace is for addition of copper to a solution of reduced apo-sBsSco. The concentration of apo-sBsSco in the reaction cell was 17 μM, and the concentration of $CuCl_2$ was 130 μM. The dotted trace is for addition of copper to oxidized apo-sBsSco. In this experiment, the concentration of apo-sBsSco was 25 μM and that of $CuCl_2$ was 500 μM. (B) The integrated heat is plotted vs the molar ratio of copper to sBsSco. The empty circles are data for reduced sBsSco, and the filled squares are data for the oxidized protein. The line through the titration of reduced sBsSco is the fit from a single-binding site model with a stoichiometry of 0.94 Cu(II) per sBsSco and an equilibrium binding constant of 1.54×10^7 M^{-1} (i.e., $K_D = 65.0$ nM). The ΔH and ΔS components were -6.94 kcal/mol and 9.88 cal mol^{-1} K^{-1}, respectively.

approached. In the next few injections, the magnitude of the signal declines in each subsequent injection to reach a value that is constant for the remainder of the titration. This value represents the heat of dilution that occurs throughout the titration. In the curve for oxidized apo-sBsSco, only the heat of dilution is observed, indicating that no specific binding interactions occur when sBsSco is oxidized. This is consistent with both the absorbance-based and fluorescence-based titrations in which there is no quenching, or absorption band formed when the cysteines of sBsSco are in the disulfide state. In Figure 6B, the integrated heat flow for each injection is plotted versus the ratio of copper to sBsSco. In each titration, the heat of dilution has been set to zero. The line through the titration of reduced sBsSco is the fit from a single-binding site model with a stoichiometry of 0.94 and an equilibrium binding constant of 1.54×10^7 M^{-1} (i.e., $K_D = 65.0$ nM). The equilibrium binding constant should be taken as an upper limit. Competition experiments will have to be conducted to determine if the true interaction between copper and sBsSco is of higher affinity than the apparent value observed here. The ΔH and ΔS components were 6.94 kcal/mol and 9.88 cal mol^{-1} K^{-1}, respectively. The binding energetics are apparent and include not only the contribution from binding of copper(II) to the protein but also any coupled changes in the protein or buffer (e.g., protonation), or that of solvent interactions with the protein and/or the metal ion. A replicate titration of another sample gave a stoichiometry of 0.87 Cu(II) per sBsSco with a K_D of 45 nM.

We have also generated a mutant of sBsSco in which the third putative copper ligand (i.e., His135) is changed to Ala (sBsScoHA) (*16*). This mutant form of sBsSco exhibits similar reactivity with reducing agents (see Table 1), and once reduced is stable in air in a manner similar to that shown above for the native protein. Therefore, the change of the conserved histidine does not alter the reducibility and stability of the reactive cysteine pair. ITC analysis of Cu(II) binding by sBsScoHA reveals a similar reaction profile as shown above for the reaction of oxidized apo-sBsSco; that is, upon addition of Cu(II) to sBsScoHA, only the heat of dilution is observed. We conclude, therefore, that the mutant has a very much lower affinity for copper. Consistent with the calorimetric analysis, addition of copper to apo-sBsScoHA does not cause a decline in the intrinsic fluorescence, or formation of an electronic or EPR absorption spectrum.

Binding of Other Metal Ions to sBsSco. We have used the fluorescence quenching assay to screen for interactions of reduced apo-sBsSco with other metal ions. Metal ions Ag(I) and Cu(I) were found to induce a strong quenching of the intrinsic fluorescence that titrated with a 1:1 stoichiometry. The Cu(I) titrations were conducted by adding a stoichiometric amount of reducing agent (i.e., either glutathione, DTT, or TCEP) to a Cu(II) solution under anaerobic conditions. Because the same quenching curve is obtained with different reductants, we conclude that the reductant is not interfering with the Cu(I)−sBsSco interaction. Zn(II), Co(II), and Ni(II) cause no change in fluorescence directly, but Co(II) in excess interfered with the interaction of sBsSco with Cu(II). Zn(II) and Ni(II) do not appear to interact with sBsSco. ITC analysis of Co(II) indicates complex formation with sBsSco with a stoichiomtery close to 1 Co(II) per sBsSco molecule and a K_D of 85 μM, or more than 1000-fold weaker than the binding of copper.

Aggregation State of Sco in Oxidized, Reduced, and Cu(II)-Bound Forms. Previously, gel filtration and multiangle light scattering were used to show that sBsSco is in a monodisperse state and that the molecular mass is in good agreement with that obtained from mass spectroscopy (*16*). Here, we have used sedimentation velocity to look at the number of species in solution for three different states of sBsSco, the oxidized apo form, the reduced apo form, and reduced sBsSco bound with Cu(II). Oxidized apo-sBsSco sediments in one major band with an S value of 2.06 ± 0.028. Integration of the sedimentation profile indicates that more than 95% of the sample is found in this band. Sedimentation of reduced apo-sBsSco and the reduced Cu(II)−sBsSco complex gives a profile that is indistinguishable from that of oxidized apo-sBsSco. We, therefore, conclude that the redox status and metalation status of sBsSco are not coupled to its aggregation state.

DISCUSSION

The Cu_A center is contained within subunit II in the cytochrome *c* oxidase subfamily of heme−copper oxidases. Cu_A receives electrons from reduced cytochrome *c* and passes them onto a low-spin heme center (i.e., cytochrome *a*) found in subunit I. SCO has been implicated as an accessory factor in the assembly of the integral membrane enzyme cytochrome *c* oxidase. Evidence from studies in yeast (*11*) and *B. subtilis* (*26*) supports a specific role in the assembly of the Cu_A center of cytochrome *c* oxidase. Several different views have been advanced for SCO's role in Cu_A assembly. SCO has been proposed to be a copper delivery agent that specifically brings copper to apo subunit II of cytochrome *c* oxidase (*29*). Alternatively, the discovery that SCO is a member of the thioredoxin family has rekindled interest in a possible redox role for SCO in Cu_A assembly (*16*). The Cu_A site includes two copper ions bridged by two thiol side chain from two cysteine residues. Presumably, the two cysteines within the Cu_A site are maintained in a reduced state because formation of a disulfide would preclude incorporation of copper into this site. SCO could then function as a thiol oxidoreductase specific for the Cu_A site. A third possibility is that SCO proteins serve in a more general role as a redox signaling molecule (*17*). In this work, we have focused on a recombinant, soluble form of SCO derived from *B. subtilis* (i.e., sBsSco). We have shown that sBsSco forms high-affinity complexes with copper and silver and that metal binding is strictly dependent on the conserved cysteine pair being in their reduced dithiol state. In addition, the third highly conserved residue (i.e., H135) is also critical for metal binding. These properties are consistent with BsSco acting as a copper delivery molecule, but whatever the ultimate redox and metal binding states, these residues are key determinants of BsSco's functional status.

Another feature of the participation of metals in biology is the specificity that proteins exhibit for binding particular metal ions. In our work, sBsSco exhibits the ability to distinguish copper from cobalt, nickel, and zinc. If copper delivery is SCO's role in vivo, then distinguishing copper from these other metals, particularly zinc, would be an important property. In the absence of a high-resolution structure for metal-bound SCO, we do not know the precise ligand geometry at the metal binding site. For Cu(II)-bound sBsSco, our spectral properties are consistent with two cysteine thiols, one imidazole nitrogen, and one water. Although further work is required to assign this spectrum in molecular detail, the form is consistent with contributions from a ligand to metal charge transfer, along with $d \rightarrow d$ transitions centered on the metal ion (*30*). Our UV−vis absorbance and rhombic EPR signal for sBsSco resemble data for the red copper site in nitrosocyanin (*31*), a protein whose sequence is homologous to those of simple blue copper proteins, but a unique electronic structure at the copper. Nitrosocyanin has both thiol and imidazole ligation.

If the ligand arrangement of sBsSco is square planar and fairly inflexible, it could explain sBsSco's preference for copper over zinc which prefers tetrahedral geometry, and over nickel and cobalt which prefer an octahedral arrangement (*32*). Alternatively, the selectivity for copper could derive from the ability of copper to induce a conformational change in sBsSco that is required for formation of the high-affinity site (*16*), and such a conformational change would not occur when sBsSco interacts with the other metals. It will be of interest to explore mutants of sBsSco to see if this metal selectivity can be tuned to a different preference.

BsSco forms stable complexes with both Cu(I) and Cu(II) ions in vitro. Our EPR and optical absorption properties of the Cu(II)−sBsSco species together with EXAFS studies on the Cu(I)−Sco complex (*12*) are consistent with an inner sphere ligand field, including two cysteine thiols and one nitrogen from histidine. The involvement of two cysteine residues is somewhat unusual as such closely spaced thiols will often form a disulfide. Copper(II) is often used to catalyze disulfide bond formation in protein-engineered, disulfide cross-linking experiments (*33*). The interaction of Cu(II) with proteins often results in the induction of an oxidation process in which the metal catalyzes electron transfer from a group on the protein to molecular oxygen. For example, in the amyloid precursor protein, two cysteines are oxidized to cystine with reduction of Cu(II) to Cu(I) (*34*), and in the prion protein, methionine is proposed to be the source of reducing equivalents for the reduction of Cu(II) to Cu(I) (*35*). These reactions are examples of the potential dangers of transition metal-catalyzed production of free radicals in biological systems which has led to the metallochaperone paradigm for escorting transition metals safely to their proper reaction sites (*36*). The stability of sBsSco metal complexes that we observe could afford SCO a role in protecting cells from the potential damaging effects that could be caused by free metal.

The reactivity of the conserved cysteine pair in sBsSco and its capacity to bind metals have been determined here for the first time. When the protein is in the reduced state, it exhibits a high affinity for Cu(II), Cu(I), and Ag(I). The dissociation constant for the Cu(II)−sBsSco complex is ~50 nM, and our results are consistent with a binding site for Cu(II) that includes two cysteine thiolates, an imidazole from histidine, and at least one water molecule. We propose that this ligation environment will change when the Cu(II) ion is reduced to Cu(I), and this may be an important aspect of Sco's function. The properties we have observed here for sBsSco are consistent with a proposed role for Sco proteins in delivering copper to the Cu_A site of cytochrome *c* oxidase. In addition, the features reported here for sBsSco would also allow Sco proteins to respond to a cell's metal content and redox state, and thus may suit Sco for a role as a redox sensor. To clarify the role of Sco in cytochrome *c* oxidase assembly, further work is required to reach a detailed understanding of this protein's interactions with metals and redox determinants within the environment of the cell.

ACKNOWLEDGMENT

We are grateful to Mr. Kim Munro of the Protein Function Discovery facility for assistance with the analytical ultracentrifuge.

REFERENCES

1. Richter, O. M., and Ludwig, B. (2003) Cytochrome *c* oxidase: Structure, function, and physiology of a redox-driven molecular machine, *Rev. Physiol. Biochem. Pharmacol. 147*, 47−74.
2. Brzezinski, P. (2004) Redox-driven membrane-bound proton pumps, *Trends Biochem. Sci. 29*, 380−387.

3. Hill, B. C. (1991) The reaction of the electrostatic cytochrome *c*-cytochrome oxidase complex with oxygen, *J. Biol. Chem. 266*, 2219−2226.
4. Pan, L. P., Hibdon, S., Liu, R. Q., Durham, B., and Millett, F. (1993) Intracomplex electron transfer between ruthenium-cytochrome *c* derivatives and cytochrome *c* oxidase, *Biochemistry 32*, 8492−8498.
5. Carr, H. S., and Winge, D. R. (2003) Assembly of cytochrome *c* oxidase within the mitochondrion, *Acc. Chem. Res. 36*, 309−316.
6. Rees, E. M., and Thiele, D. J. (2004) From aging to virulence: Forging connections through the study of copper homeostasis in eukaryotic microorganisms, *Curr. Opin. Microbiol. 7*, 175−184.
7. Luk, E., Jensen, L. T., and Culotta, V. C. (2003) The many highways for intracellular trafficking of metals, *J. Biol. Inorg. Chem. 8*, 803−809.
8. Beers, J., Glerum, D. M., and Tzagoloff, A. (1997) Purification, characterization, and localization of yeast Cox17p, a mitochondrial copper shuttle, *J. Biol. Chem. 272*, 33191−33196.
9. Maxfield, A. B., Heaton, D. N., and Winge, D. R. (2004) Cox17 is functional when tethered to the mitochondrial inner membrane, *J. Biol. Chem. 279*, 5072−5080.
10. Schulze, M., and Rodel, G. (1989) Accumulation of the cytochrome *c* oxidase subunits I and II in yeast requires a mitochondrial membrane-associated protein, encoded by the nuclear SCO1 gene, *Mol. Gen. Genet. 216*, 37−43.
11. Glerum, D. M., Shtanko, A., and Tzagoloff, A. (1996) SCO1 and SCO2 act as high copy suppressors of a mitochondrial copper recruitment defect in *Saccharomyces cerevisiae*, *J. Biol. Chem. 271*, 20531−20535.
12. Nittis, T., George, G. N., and Winge, D. R. (2001) Yeast Sco1, a protein essential for cytochrome *c* oxidase function, is a Cu(I)-binding protein, *J. Biol. Chem. 276*, 42520−42526.
13. Beers, J., Glerum, D. M., and Tzagoloff, A. (2002) Purification and characterization of yeast Sco1p, a mitochondrial copper protein, *J. Biol. Chem. 277*, 22185−22190.
14. Andrews, D., Rattenbury, J., Anand, V., Mattatall, N. R., and Hill, B. C. (2004) Expression, purification, and characterization of BsSco, an accessory protein involved in the assembly of cytochrome *c* oxidase in *Bacillus subtilis*, *Protein Expression Purif. 33*, 57−65.
15. Balatri, E., Banci, L., Bertini, I., Cantini, F., and Ciofi-Baffoni, S. (2003) Solution structure of Sco1: A thioredoxin-like protein involved in cytochrome *c* oxidase assembly, *Structure 11*, 1431−1443.
16. Ye, Q., Imriskova-Sosova, I., Hill, B. C., and Jia, Z. (2005) Identification of a disulfide switch in BsSco, a member of the Sco family of cytochrome *c* oxidase assembly proteins, *Biochemistry 44*, 2934−2942.
17. Williams, J. C., Sue, C., Banting, G. S., Yang, H., Glerum, D. M., Hendrickson, W. A., and Schon, E. A. (2005) Crystal structure of human SCO1: Implications for redox signaling by a mitochondrial cytochrome *c* oxidase "assembly" protein, *J. Biol. Chem. 280*, 15202−15211.
18. Imriskova-Sosova, I., Ye, Q., Hill, B. C., and Jia, Z. (2003) Purification, crystallization and preliminary X-ray analysis of a Sco1-like protein from *Bacillus subtilis*, a copper-binding protein involved in the assembly of cytochrome *c* oxidase, *Acta Crystallogr. D59*, 1299−1301.
19. Ciriolo, M. R., Desideri, A., Paci, M., and Rotilio, G. (1990) Reconstitution of Cu,Zn-superoxide dismutase by the Cu(I)•glutathione complex, *J. Biol. Chem. 265*, 11030−11034.
20. Lakowicz, J. R. (1999) *Principles of Fluorescence Spectroscopy*, Plenum, New York.
21. Dam, J., and Schuck, P. (2004) Calculating sedimentation coefficient distributions by direct modeling of sedimentation velocity concentration profiles, *Methods Enzymol. 384*, 185−212.
22. Riener, C. K., Kada, G., and Gruber, H. J. (2002) Quick measurement of protein sulfhydryls with Ellman's reagent and with 4,4′-dithiodipyridine, *Anal. Bioanal. Chem. 373*, 266−276.
23. Holmgren, A. (1979) Thioredoxin catalyzes the reduction of insulin disulfides by dithiothreitol and dihydrolipoamide, *J. Biol. Chem. 254*, 9627−9632.
24. Erlendsson, L. S., Acheson, R. M., Hederstedt, L., and Le Brun, N. E. (2003) *Bacillus subtilis* ResA is a thiol-disulfide oxidoreductase involved in cytochrome *c* synthesis, *J. Biol. Chem. 278*, 17852−17858.
25. Chen, Y., and Barkley, M. D. (1998) Toward understanding tryptophan fluorescence in proteins, *Biochemistry 37*, 9976−9982.
26. Mattatall, N. R., Jazairi, J., and Hill, B. C. (2000) Characterization of YpmQ, an accessory protein required for the expression of cytochrome *c* oxidase in *Bacillus subtilis*, *J. Biol. Chem. 275*, 28802−28809.
27. Cline, D. J., Redding, S. E., Brohawn, S. G., Psathas, J. N., Schneider, J. P., and Thorpe, C. (2004) New water-soluble phosphines as reductants of peptide and protein disulfide bonds: Reactivity and membrane permeability, *Biochemistry 43*, 15195−15203.
28. Peisach, J., and Blumberg, W. E. (1974) Structural implications derived from the analysis of electron paramagnetic resonance spectra of natural and artificial copper proteins, *Arch. Biochem. Biophys. 165*, 691−708.
29. Lode, A., Kuschel, M., Paret, C., and Rodel, G. (2000) Mitochondrial copper metabolism in yeast: Interaction between Sco1p and Cox2p, *FEBS Lett. 485*, 19−24.
30. Solomon, E. I., Lowery, M. D., LaCroix, L. B., and Root, D. E. (1993) Electronic absorption spectroscopy of copper proteins, *Methods Enzymol. 226*, 1−33.
31. Basumallick, L., Sarangi, R., DeBeer, G. S., Elmore, B., Hooper, A. B., Hedman, B., Hodgson, K. O., and Solomon, E. I. (2005) Spectroscopic and density functional studies of the red copper site in nitrosocyanin: Role of the protein in determining active site geometric and electronic structure, *J. Am. Chem. Soc. 127*, 3531−3544.
32. Rulisek, L., and Vondrasek, J. (1998) Coordination geometries of selected transition metal ions (Co^{2+}, Ni^{2+}, Cu^{2+}, Zn^{2+}, Cd^{2+}, and Hg^{2+}) in metalloproteins, *J. Inorg. Biochem. 71*, 115−127.
33. Rodgers, A. J., and Capaldi, R. A. (1998) The second stalk composed of the β- and δ-subunits connects F0 to F1 via an α-subunit in the *Escherichia coli* ATP synthase, *J. Biol. Chem. 273*, 29406−29410.
34. Multhaup, G., Schlicksupp, A., Hesse, L., Beher, D., Ruppert, T., Masters, C. L., and Beyreuther, K. (1996) The amyloid precursor protein of Alzheimer's disease in the reduction of copper(II) to copper(I), *Science 271*, 1406−1409.
35. Wong, B. S., Wang, H., Brown, D. R., and Jones, I. M. (1999) Selective oxidation of methionine residues in prion proteins, *Biochem. Biophys. Res. Commun. 259*, 352−355.
36. Valentine, J. S., and Gralla, E. B. (1997) Delivering copper inside yeast and human cells, *Science 278*, 817−818.

BI051343I